

1
2
3
4
5
6
7
8
9
10
11
12
13
14
15
16
17
18
19
20
21

Ethylene glycol intercalation in smectites. Molecular dynamics simulation studies

Marek Szczerba^{1*}, Zenon Kłapyta² Andrey Kalinichev³

¹Institute of Geological Sciences, Polish Academy of Sciences, Kraków, Poland

²Faculty of Geology, Geophysics and Environmental Protection,

University of Mining and Metallurgy, Kraków, Poland

³Laboratoire SUBATECH, Ecole des Mines de Nantes, Nantes, France

* Corresponding author :

E-mail : ndszcer@cyf-kr.edu.pl; tel: +48 12 3705232; fax: +48 12 4221609

22 **Abstract**

23

24 Molecular dynamics simulations were performed in order to study the interactions of
25 ethylene glycol (EG) with smectite. The simulations have also taken into account that EG-
26 smectite complex contains, as a rule, some adsorbed water molecules. The simulations results
27 show that in the two-layer glycolate the content of water is of about 1.0 H₂O per half of the
28 smectite unit cell. For a typical smectite a clear thermodynamic preference for one- or two-
29 layer structure of the complexes is observed. The calculated radial distribution functions and
30 running coordination numbers indicate that the H₂O and EG molecules compete for the
31 coordination sites near the calcium ions in the clay interlayers. The EG and H₂O packing in
32 the interlayer space is controlled by the differences in the total smectite layer charge, charge
33 distribution, and the type of the interlayer cation, strongly affecting the basal spacing and the
34 structure of the complex. Varying amounts of EG and water and the ratio EG/H₂O are,
35 however, the most important factors influencing the extent of the smectite expansion.

36 A comparison of the two-layer structure obtained from MD simulations with previous
37 models leads to the conclusion that the arrangement of EG molecules in the interlayers,
38 typically used in simulations of clay X-ray diffractograms, can be modified. In contrast to the
39 earlier Reynolds model (1965), the main difference is that the interlayer ions tend to change
40 their positions depending on the specific distribution of the clay charge. In the case of
41 montmorillonite, Ca²⁺ ions are located in the middle of the interlayer space, while for
42 beidellite they are located much closer to the clay surface. Water molecules in this structure
43 do not form distinct layers but are instead spread out with a tendency to be concentrated
44 closer to the interlayer ions and to the smectite surface. One-layer structure of EG/water-
45 smectite complex, characteristic of vermiculite is also proposed.

46

47 1. Introduction

48

49 The intercalation of ethylene glycol (EG) in smectites (glycolation) is widely used to
50 discriminate smectites and vermiculites from other clays and from each other. During this
51 process, EG molecules penetrate into the interlayer spaces of the swelling clays, leading to the
52 formation of a two-layer structure ($\sim 17 \text{ \AA}$) in the case of smectites, or a one-layer structure
53 ($\sim 14 \text{ \AA}$) in the case of vermiculites. Although this technique has been known since the
54 pioneering work of MacEvan (1946), the arrangement of glycol molecules between smectite
55 layers is still not fully ascertained.

56 The X-ray work of Reynolds (1965) gave some insights, providing a simplified
57 structure of two-layer EG/water-smectite complex. In this structure, the interlayer Ca^{2+}
58 cations, solvated by water, are located in the middle of the interlayer space between two
59 layers of 1.7 $\text{CH}_2\text{-OH}$ on each sides of the mid-plane. This gives together 1.7 EG molecules
60 on each side, ie. 3.4 EG puc or 1.7 EG phuc. This EG structure together with 0.8
61 $\text{H}_2\text{O}/\text{O}_{10}(\text{OH})_2$ forms EG/water/smectite complex having basal spacing of 16.9-17.0 \AA .
62 Bradley et al. (1963) presented a structure of EG-vermiculite complex which contains a single
63 layer of the alcohol surrounded by sodium cations in the middle of the interlayer. The ratio
64 between EG and vermiculite is two molecules per unit cell, while no water in the structure
65 was assumed.

66 Further studies were focused on the effects of the interlayer ions and localization of
67 the layer charge on the d -spacing of EG/water-clay complexes. It was confirmed that the basal
68 spacing is larger for clay minerals with lower layer charge, but it also depends on the source
69 of the charge, the type of the exchangeable cations, the particle size and the relative humidity
70 (Harward and Brindley, 1965; Brindley, 1966; Harward et al., 1969; Środoń, 1980; Sato et al.,
71 1992). Variable basal spacing of two-layer glycol complex was taken into account in the

72 techniques of measuring the layer ratio in illite-smectites (Środoń, 1980, 1981, 1984). The
73 charge location in the tetrahedral sheet leads to lower values of basal spacing and to a
74 different behavior upon solvation, than those observed when the charge is located in the
75 octahedral layer. Moreover, it was found that smectites may form a one-layer glycol complex
76 instead of the two-layer complex at very low relative humidity (Eberl et al., 1987), or even at
77 intermediate humidity values but with K^+ as the exchange cation (Eberl et al., 1986).

78 More recently, Mosser-Ruck et al. (2005) have demonstrated several differences and
79 inconsistencies between the methods of saturation with EG, suggesting that this procedure
80 should be somehow standardized. The dynamics of glycolation for smectites saturated with
81 different cations and equilibrated from various hydrates was studied by Svensson and Hansen
82 (2010). It was found that during the reaction, a redistribution of H_2O molecules in the sample
83 took place and higher hydrates were formed, proceeding to the formation of a two-layer
84 structure of EG. This effect depends on the partial pressure of water and on the nature of the
85 exchangeable interlayer cation. It can be attributed to the higher concentration of water in the
86 interlayer space due to its substitution by EG.

87 In spite of the relatively abundant literature on the understanding and characterization
88 of the EG/water-clays complex, in the contemporary computer programs which simulate the
89 structures of smectite and illite-smectite from X-ray diffraction (XRD) data, the simplified
90 structure of this complex developed by Reynolds (1965) is still widely used. The one-layer
91 structure is only approximated, e.g. assuming interlayer cation and EG lying in the middle of
92 interlayer spaces.

93 The present study was undertaken in order to investigate the structure of EG/water-
94 clays complex in more detail using molecular dynamics (MD) simulations. It is focused on
95 such important questions as: (i) does the structure proposed by Reynolds (1965) finds a
96 confirmation in MD simulations; (ii) how much water is co-adsorbed with EG; (iii) how this

97 water is distributed in the clay interlayers; (iv) should the magnitude of clay basal spacing be
98 attributable purely to the varying amounts of EG and water in the interlayer, or the varying
99 thickness of the EG/water complex should also play a role?

100

101 **2. Methods**

102

103 The structural models of smectites were built on the basis of pyrophyllite crystal
104 structure (Lee and Guggenheim, 1981), where several isomorphic substitutions were
105 introduced at particular atomic sites. In most simulations, the structural model assumed the
106 following composition, considered as the most common in the mixed layer clays (Środoń et
107 al. 2009):



109

110 Additional simulations were also performed for pure montmorillonite and beidellite with
111 particular charges of 0.3 and 0.5 per half of the smectite unit cell (thereafter phuc). All these
112 structures were built by substituting the relevant number of Al atoms with Mg and Si with Al.
113 For all the models, the Mg/Fe/Al ordering in the octahedral sheets was set following the work
114 of Ortega-Castro et al. (2010). The Al for Si substitutions in tetrahedral sheet were randomly
115 distributed following the Löwenstein rule, which states that Al-O-Al linkages are excluded.
116 The simulation supercell was built as $8 \times 4 \times 2$ unit cells in the a , b , and c crystallographic
117 directions, respectively. This resulted on the simulated system size of $ca\ 41.6\text{\AA} \times 36.1\text{\AA} \times X\text{\AA}$.
118 The value of X varied depending on the amount of EG and water in the interlayer spaces.

119 The partial atom charges and other parameters of interatomic interactions of the
120 smectite layers were described using the CLAYFF force field (Cygan et al., 2004), which has
121 already proven itself quite successful in describing many clay-related systems in good

122 agreement with available diverse experimental data (e.g., Cygan et al., 2009; Suter and
123 Coveney, 2009; Striolo, 2011; Michot et al., 2012; Marry et al., 2013). For the H₂O and EG
124 molecules the flexible SPC model (Berendsen et al., 1981, Teleman, et al., 1987) and the
125 AMBER (Hornak et al., 2006) force field were used, respectively. Ewald summation was
126 applied to calculate the long range corrections to the Coulombic interactions (e.g., Frenkel
127 and Smit, 2002) and the cutoff distance was set to 8.5 Å.

128 The structural models of EG/water-smectite complexes were constructed using the
129 Monte Carlo approach with the help of the Towhee computer program
130 (<http://towhee.sourceforge.net>). For these initial structures, energy minimizations were
131 performed first, followed by *NPT*-ensemble MD simulations at 1 bar in temperature cycles
132 using Langevin dynamics to control the temperature and Langevin piston to control the
133 pressure. The time step to integrate the equations of atomic motion was set at 0.001 ps and the
134 dynamic trajectories of all atoms and system properties were recorded every 1 ps. During the
135 first period of every cycle, the temperature was set at 700 K and the simulation was run for
136 150 ps. Then the temperature was dropping in steps of 50 K, with short 10 ps equilibration
137 MD runs at each step until the temperature reached 300 K. After that, each simulation
138 continued at 300 K for 250 ps for which the equilibrium system properties were recorded for
139 further analysis. Each cycle was repeated from two time origins (?), depending on the type of
140 calculation. In the calculations of *z*-density profiles, one atom of the octahedral sheet was
141 fixed at its initial position. However, its interactions with neighboring atoms were fully
142 calculated during the simulation. All MD simulations were performed using the LAMMPS
143 computer program (Plimpton, 1995).

144

145 **3. Results and discussion**

146

147 **3.1. EG/water-smectite complex with variable content of EG**

148

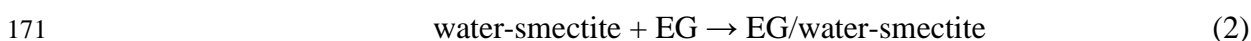
149 Experimental data show substantial preference for the formation of the EG/water-
150 smectite complex as a two-layer structure, especially when solvated with liquid EG (e.g.
151 Mosser-Ruck et al., 2005). It is therefore interesting to investigate the mechanism of this
152 process, the thermodynamics of reaction, variation of the basal spacing and the structure of
153 the complex.

154 In the present study, MD simulations with constant number of water molecules and
155 varying number of EG molecules were performed for a smectite with the composition
156 according to Środoń et al. (2009). The number of interlayer water molecules was set,
157 according to Reynolds (1965), at 0.8 H₂O phuc.

158 The calculated evolution of the basal spacing (Fig. 1) confirms the formation of two
159 possible structures: one- and two-layer complexes. The one-layer structure is well defined,
160 marked with a plateau of the basal spacing at ca. 14 Å. This value corresponds to the
161 composition of 0.8 EG/O₁₀(OH)₂, while for 1.0 EG/O₁₀(OH)₂ the basal spacing is even
162 slightly above 14 Å. The two-layer structure is less defined and its basal spacing is in the
163 range between 16.8 Å and 17.3 Å for the compositions of 1.7 EG/O₁₀(OH)₂ and
164 1.9 EG/O₁₀(OH)₂, respectively. These values explain the relatively large variability of the
165 basal spacing, which depends on the mode of the complex preparation. The resulting basal
166 spacing values also correspond very well with the values obtained by Reynolds (1965) who
167 found them in the range of 16.9-17.0 Å for 0.8 H₂O/O₁₀(OH)₂ and 1.7 EG/O₁₀(OH)₂.

168 In order to study the thermodynamics of the glycolation process, the following
169 reaction was considered:

170



172

173 The calculation of ΔE for this reaction required computation of the potential energy of pure
174 EG. For this purpose, a EG simulation box consisting of 330 molecules was built and
175 equilibrated. Its potential energy was calculated with the same approach as used for the
176 simulations of the complexes. The resulting value equals to 11.672 ± 0.006 kcal/mol.

177 The plot of ΔE for the reaction (2) (Fig. 2) shows two minima: a local one at
178 ~ 1.0 EG/O₁₀(OH)₂ (corresponding to the one-layer structure) and a second global one at
179 ~ 1.8 EG/O₁₀(OH)₂ (corresponding to the two-layer structure). The respective values of the
180 basal spacing are equal to ~ 14.3 Å and ~ 17.0 Å, which agrees well with experimental data.
181 The reaction of formation of the two-layer structure has much lower value of ΔE , indicating a
182 strong preference for the formation of the two-layer structure for typical smectite. It should be
183 noted, however, that ΔE is just the internal energy, not the Gibbs free energy of reaction.
184 Therefore, the results cannot be directly applied for the prediction of chemical equilibria,
185 because they do not take entropic factors into account.

186 To quantitatively assess the molecular mechanism of the EG/water-smectite complex
187 formation, the atom-atom radial distribution functions (RDF) and the corresponding running
188 coordination numbers (RCN) were calculated. The shape of the RCN obtained for the
189 interlayer Ca²⁺ ion and the oxygen atom of EG (O_{EG}) (Fig. 3a) shows that with increasing
190 number of EG molecules in the interlayer space, the number of O_{EG} atoms coordinated to Ca²⁺
191 ions atoms also increases. This effect can be attributed mainly to the gradual filling of the
192 interlayer space around these ions, with simultaneous expulsion of water molecules from the
193 neighborhood of Ca²⁺ ions and thus from the interlayer spaces. This is confirmed by the shape
194 of the RCN calculated for Ca²⁺ ions and oxygen atoms of water (O_w) (Fig. 3b). The
195 increasing number of EG molecules leads to the decrease in the number of water molecules in

196 the ion coordination spheres. This effect finds its confirmation in the study of Svensson and
197 Hansen (2010).

198 One important result visible in the RDF plots is that the dominating distance between
199 calcium ions and oxygen atoms of EG (Ca-O_{EG}) is 2.45 Å, which is almost identical to the
200 typical distances between calcium ions and oxygens of water (Ca-O_{W}). These values are
201 almost the same in spite of the structural differences between the complexes formed by both
202 of these molecules with calcium ions (Fig. 4), and do not depend on the number of EG
203 molecules in the interlayer space. Some differences are only visible at very low EG content in
204 the complex in the form of slight shift of both Ca-O_{EG} and Ca-O_{W} dominating distances by
205 about 0.025 Å. In the case of EG, the cis conformation generally dominates, with two oxygen
206 atoms coordinated to the calcium ion. Thus a chelate complex is formed. In contrast, water
207 molecule contains only one negative oxygen atom and therefore the structure of hydrated Ca^{2+}
208 is simpler.

209

210 **3.2. Two-layer EG/water-smectite complex with varying water content**

211

212 The original Reynolds (1965) study and further experimental evidences, like, e.g.,
213 variability of basal spacing of two-layer EG-smectite complex depending on relative humidity
214 (Hsieh, 1989), indicate that the complex EG-smectite contains water. In order to study this
215 effect, the EG-smectite complex containing a constant number of EG molecules:

216 1.7 EG/ $\text{O}_{10}(\text{OH})_2$ (after Reynolds, 1965) was simulated with variable amounts of water.

217 The plot of clay basal spacing versus variable water content (Fig. 5) indicates that,
218 with increasing number of water molecules, the basal spacing increases more or less linearly.
219 However, for the structures with very low water content the value of basal spacing does not
220 change. This plateau corresponds to ~16.5 Å. These results confirm the data of Hsieh (1989),

221 who observed a relatively linear relationship between relative humidity and the basal spacing,
222 and indicate that the amount of water in EG/water-smectite complex may vary.

223 In order to calculate the thermodynamics of the hydration reaction of EG-smectite
224 complex, the value of ΔE of the following reaction was calculated:

225



227

228 The potential energy of water was taken into account by a separate MD simulation for a water
229 box consisting of 508 molecules. The resulting value is -9.83 ± 0.08 kcal/mol. Within the
230 statistical accuracy, this value is identical to the value of -9.8823 kcal/mol calculated for the
231 SPC water model by Mark and Nilsson (2001). The values of ΔE for the reaction (3) for
232 different water contents in the EG-smectite complex (Fig. 6) indicate that the most probable
233 content of H₂O in this complex with EG is 1.0 phuc. This value corresponds quite well to the
234 value of 0.8 calculated by Reynolds (1965). It should be noted, however, that the hydration
235 levels of the complex can vary in a relatively broad range, so it should be taken into account
236 both in the standardization of the preparation procedure of EG/water-smectite complex and in
237 the modeling and refinement of the XRD data. It should be also noted that the obtained
238 estimates are only semi-quantitative because, as it was mentioned above, the entropic factors
239 were not taken into account.

240 Radial distribution functions and running coordination numbers provide further
241 insights into the mechanism of EG and water co-adsorbition in smectite. From the RDF
242 obtained for the pair of Ca²⁺ ion and O_{EG} (Fig. 7a) it is visible that the oxygen atoms are
243 located at the distance of ~ 2.45 Å from the calcium ions. The second maximum at ~ 4.6 Å,
244 which corresponds to the second coordination sphere, is of very small height. The increasing
245 water content in the structure leads to the lowering of the coordination number of O_{EG} around

246 calcium ions, which is visible in the RCN plots (Fig. 7a). This indicates that water partially
247 expels EG molecules from the close neighborhood of the calcium ions in the interlayer space.
248 This finds further confirmation in the shape of the RCN calculated for Ca^{2+} ion and the
249 oxygen of water (O_W) (Fig. 7b). The more water in the structure, the higher the running
250 coordination number for the Ca^{2+} - O_W pair is. Independent on the water content in the
251 structure, RDF plots show that the O_W and O_{EG} are located in the first coordination sphere of
252 Ca^{2+} at the distance of $\sim 2.45 \text{ \AA}$. A comparison of these results with Fig. 3 indicates that EG
253 and water molecules compete for the coordination of calcium ions in the smectite interlayers.

254

255 **3.3. Two-layer EG/water-smectite complex with different smectites**

256

257 Many previous studies have shown that the basal spacing of the EG/water-smectite
258 complex varies depending on the layer charge and its source/location (e.g., Sato et al., 1992).
259 Therefore, it is interesting to check if the basal spacing will differ for different smectites in
260 the case of the same/fixed amounts of EG and water in the interlayer. These values were set
261 after Reynolds (1965) at 0.8 H_2O and 1.7 EG phuc. Beidellite and montmorillonite with the
262 layer charge of 0.3 and 0.5 phuc were chosen.

263 The results show that the basal spacing varies in a very broad range – visibly higher
264 values are reached for smectites with lower charges (Table 1). Taking into account the
265 uncertainty of the basal spacing calculation, the obtained values do not depend much on the
266 location of the charge. Therefore, the experimentally found differences in the basal spacing
267 between beidellite and montmorillonite (e.g., Sato et al., 1992) should be attributed to the
268 differences in the amounts of adsorbed EG and water.

269 Although the location of the charge does not have substantial influence on the basal
270 spacing, its impact on the structure of the EG/water-smectite complex is very important (Fig.

271 8). In the case of beidellite, which has layer charge located entirely in the tetrahedral sheet,
272 Ca^{2+} ions tend to be adsorbed close to the surface (Fig. 8a, b). For low charge
273 montmorillonite, Ca^{2+} ions are located generally in the middle of the interlayer (Fig. 8c). In
274 the case of montmorillonite with higher charge, the tendency of ions to be adsorbed closer to
275 the surface is visible. However, a lot of ions are still located in the middle of the interlayer
276 space (Fig. 8d).

277

278 **3.4. Two-layer EG/water-smectite complex with different interlayer ions**

279

280 The nature of the interlayer cation was found to affect the structure of the EG/water-
281 smectite complexes (e.g. Sato et al., 1992). Potassium-saturated and ammonium-saturated
282 smectites with low layer charge show the highest basal spacing after glycolation, much higher
283 than, e.g., their sodium- or calcium- saturated analogues (Środoń, 1980). For high-charge K-
284 smectites the one-layer structure is observed (Eberl et al., 1986). The transition from the two-
285 layer to one-layer structure clearly reflects the variable amounts of EG and water in the
286 interlayer. The variation in the basal spacing of the two-layer complex may be due to different
287 factors. To investigate this effect, smectites with the same contents of EG and water and with
288 different interlayer cations were simulated (Table 2).

289 The results confirm the experimental data (Środoń, 1980) that the basal spacing is
290 higher for monovalent cations, which seems to be generally intuitive because of the two
291 reasons:

292 - larger ion radius of these ions,

293 - two times higher content of the monovalent cations that balances the same negative charge
294 of smectite.

295 However, there is also a distinct variability of the basal spacing in the case of
296 monovalent cations. For potassium this value is very high: 17.08 Å, in contrast to 16.859 Å
297 for sodium. This effect can be explained partially by the larger ion radius of potassium, but it
298 also reflects a different interlayer structure, namely the fact that potassium ions tend to
299 concentrate closer to the clay surface, because of their lower hydration energy than that of the
300 sodium ions, which tend to concentrate in the middle of interlayers (Fig. 9). Additionally, Na⁺
301 ions, due to their relatively small size, can deeper penetrate the pseudohexagonal gaps in the
302 tetrahedral sheets, which can also affect the basal spacing.

303

304 **3.5. Comparison of MD-simulated structures with previous experimental data**

305

306 One of the most important objectives of this work was to check if the structure of the
307 EG-smectite complex obtained from the Fourier analysis of the experimental X-ray data
308 (Reynolds, 1965) agrees with the results of molecular dynamics simulations. The
309 experimental structure was obtained for low charge montmorillonite (ca. 0.33 phuc), therefore
310 the results calculated for montmorillonite with the layer charge of 0.3 were taken for
311 comparison. Due to the fact that from XRD analysis of oriented specimens it is very difficult
312 to discriminate the type of atoms contributing to the electronic density, the MD profile was
313 transformed into electronic density profiles. The interlayer configurations of Reynolds (1965)
314 were transformed taking into account temperature factors *B*. The relation between the *B* factor
315 and the full-width at half maximum intensity of the Gaussian distribution was calculated from
316 equation (e.g. Dazas et al., 2013):

317

$$FWHM = \frac{\sqrt{B} \sqrt{\ln(2)}}{\pi} \quad (4)$$

318

319 The electronic density profiles resulting from the MD simulation show some
discrepancies in comparison to the suggested electronic distribution of Reynolds (1965)

320 structure (Fig. 10). The position of EG from Reynolds (1965) agrees quite well with that of
321 MD simulations (EG is considered as a sum of contributions from its carbon and oxygen
322 atoms). According to the MD simulations, calcium ions are mostly located close to the middle
323 of the interlayer (two maxima of the thick solid line near ~ -0.7 Å and $+0.7$ Å), which is in
324 agreement with the Reynolds model. The largest difference between the results of MD
325 simulations and those obtained from the Fourier analysis of experimental XRD data is the
326 position of water molecules, which tend to concentrate closer to the smectite surface and not
327 in the middle of the interlayer space. Generally, comparisons of the total electronic density
328 profiles (thick lines in Fig. 10) show very small difference in the contributions of EG but
329 much larger differences in the middle of the interlayer occupied by cations and water. This
330 indicates that, although the structure of Reynolds (1965) has been successfully used to model
331 EG/water/smectite complexes, some improvement of this structure is possibly necessary.

332 In the case of smectites with different values and localizations of the charge, the
333 discrepancy between the MD results and experimental data (Reynolds, 1965) are much more
334 apparent (Fig. 8). This indicates that the experimental EG/water-smectite structure can be
335 applicable only to some specific types of smectites (i.e., montmorillonite with low charge). In
336 other cases, different atomic distributions should be used in the modeling of XRD data.

337 It was found experimentally that EG can form one-layer structure and also mixed
338 layered structures, composed of one- and two-layered ones. Because of the absence of a good
339 model for the EG one-layer complex, it was important to study this structure and propose such
340 a model.

341 To build this structure, the composition of 1.0 EG/O₁₀(OH)₂ and 0.8 H₂O/O₁₀(OH)₂
342 (corresponding to local minimum in Fig. 2) in the interlayer space were assumed. The typical
343 smectite structure of Środoń et al. (2009) was taken into account. For the EG atoms (Fig. 11)
344 two maxima are visible on both sides from the middle of the interlayer: one is due to the

345 carbon atoms, while the second one - due to the oxygen atoms located closer to the surface
346 and to the calcium ions. Ca^{2+} ions are mainly located in the middle of the interlayer space.
347 Water molecules tend to coordinate the calcium ions and basal oxygens of the clay surface.

348 A comparison of total electronic density profile with the density profile of Bradley et
349 al. (1961) shows substantial differences (Fig. 12). These are related to the fact that Bradley et
350 al. (1961) obtained their structure for vermiculite, which has on average two times larger layer
351 charge than a typical smectite, and also for dry EG. Water molecules should, however, be
352 assumed to be present in the structure, as can be found in the data of Hsieh (1989). Important
353 difference lies also in the basal spacing of these two structures: 12.9 Å for Bradley et al.
354 (1961) and 14.3 Å for studied structure. It should therefore be noted that the obtained
355 structure does not correspond to the structure of complex in vermiculite but can rather be
356 related to the one-layer contribution in mixed one- and two- layered EG smectite complexes.

357

358 **4. Summary and Conclusions**

359

360 The results of molecular dynamics simulations of EG/water-smectite complexes were
361 compared to the earlier experimental data. The thermodynamic preference of two-layer
362 structures was confirmed by the simulations. The water content in the EG/water-smectite
363 complexes is estimated to be close to 1.0 H_2O phuc. Generally, H_2O and EG molecules
364 compete for the coordination sites around Ca^{2+} ions in the interlayers.

365 The simulation results allow us to conclude that the model structure used for over 40
366 years in the interpretation of XRD measurements of smectites and illite-smectites (Reynolds,
367 1965) should be revised. EG forms two distinct layers between the silicate sheets, but the
368 interlayer ions can form both inner- and outer-sphere complexes with water, not only the
369 outer-sphere ones as it was previously assumed. Water molecules in this structure are found

370 not only to concentrate close to the calcium ions in the middle of the interlayer, but also to
371 adsorb closer to the clay surface, like the EG. An atomistically detailed model of the one-
372 layer complex is also proposed based on the MD simulations.

373 It was confirmed that the thickness of the glycol complex strongly depends both on the
374 nature of the interlayer cation and on the total layer charge, but to a lesser extent also on the
375 charge location. Therefore, this variable thickness of the complex has to be taken into account
376 in the XRD pattern modeling.

377 One has to bear in mind, however, that any results of molecular simulations are, to
378 some extent, force field dependent. The CLAYFF (Cygan et al., 2004) used in our present
379 work has already proven itself among the best performing force field parameterizations for
380 many clay-related simulations (e.g., Heinz et al., 2005; Striolo, 2011; Michot et al., 2012;
381 Marry et al., 2013). Nevertheless, new improvements are continued to be made. In particular,
382 a new INTERFACE force field, specifically designed to model organo-inorganic clay-related
383 nanostructures has been published when this paper was already under revision (Heinz et al.,
384 2013). Its application in our future studies of the smectite-EG systems should be expected to
385 further improve the currently presented results and make them more quantitatively accurate.

386

387 **5. References**

388

389 Berendsen, H.J.C., Postma, J.P.M., van Gunsteren, W.F., Hermans, J. (1981) Interaction models for water in
390 relation to protein hydration. In *Intermolecular Forces*; Pullman, B., Ed.; D. Reidel: Amsterdam, pp 331

391

392 Bradley W. F., Weiss E. J. and Rowland R. A. (1963) A glycol sodium vermiculite complex. *Clays and Clay*
393 *Miner.* 10, 117-122

394

395 Brindley G.W. (1966) Ethylene glycol and glycerol complexes of smectite and vermiculites. *Clay Minerals.* 6,
396 237-259

397

398 Cygan, R. T., Liang, J. J., and Kalinichev, A. G. (2004) Molecular models of hydroxide, oxyhydroxide, and clay
399 phases and the development of a general force field. *Journal of Physical Chemistry B*, 108, 1255-1266.
400

401 Cygan R. T., Greathouse J. A., Heinz H., and Kalinichev A. G. (2009) Molecular models and simulations of
402 layered materials. *Journal of Materials Chemistry* 19, 2470-2481.
403

404 Eberl D. D., Środoń J. and Northrop H. R. (1986) Potassium fixation in smectite by wetting and drying. In: J.A.
405 Davis and K.F. Hayes, eds. *Geochemical Processes at Mineral Surfaces*, American Chemical Society
406 Symposium Series 323, 296-326.
407

408 Eberl D. D., Środoń J., Lee M., Nadeau P. H. and Northrop H. R. (1987) Sericite from the Silverton caldera,
409 Colorado: Correlation among structure, composition, origin, and particle thickness. *Am. Mineral.* 72, 914-934.
410

411 Ferrage E., Lanson B., Michot L. J. and Robert J.-L. (2010) Hydration Properties and Interlayer Organization of
412 Water and Ions in Synthetic Na-Smectite with Tetrahedral Layer Charge. Part 1. Results from X-ray Diffraction
413 Profile Modeling. *J. Phys. Chem. C.* 114, 4515–4526
414

415 Frenkel, D. and Smit, B. (2002) *Understanding Molecular Simulation: From Algorithms to Applications*.
416 Academic Press, San Diego, 638 pp.
417

418 Harward M.E. and Brindley G.W. (1965) Swelling properties of synthetic smectite in relation to lattice
419 substitutions. *Clays and Clay Minerals.* 13, 209-222
420

421 Harward M.E., Carstea D.D. and Sayegh A.H. (1969) Properties of vermiculite and smectites: Expansion and
422 collapse. *Clays and Clay Minerals*, 16, 437-447
423

424 Heinz H., Koerner H., Anderson K. L., Vaia R. A., and Farmer B. L. (2005) Force field for mica-type silicates
425 and dynamics of octadecylammonium chains grafted to montmorillonite. *Chemistry of Materials* 17, 5658-5669.
426

427 Heinz, H., Lin, T. J., Mishra, R. K., and Emami, F. S. (2013) Thermodynamically consistent force fields for the
428 assembly of inorganic, organic, and biological nanostructures: The INTERFACE force field. *Langmuir* 29,
429 1754–1765.

430

431 Hsieh Y.P. (1989) Effects of relative humidity on the basal expansion of Mg-smectite equilibrated with ethylene
432 glycol at low vapor pressure. *Clays and Clay Minerals*, 37, 459-463

433

434 Hornak V, Abel R, Okur A, Strockbine B, Roitberg A, and Simmerling C. (2006) Comparison of multiple
435 Amber force fields and development of improved protein backbone parameters. *Proteins*. 65, 712-25

436

437 Lee J. H. and Guggenheim S. (1981) Single crystal X-ray refinement of pyrophyllite-1Tc. *American*
438 *Mineralogist*. 66, 350-357

439

440 Liu, X.D., Lu, X.C., Wang, R.C. and Zhou, H.Q. (2008) Effects of layer-charge distribution on the
441 thermodynamic and microscopic properties of Cs-smectite. *Geochim. Cosmochim. Acta*, 72, 1837-1847

442

443 MacEwan D. M. C. (1946) The identification and estimation of montmorillonite group of minerals, with special
444 reference to soil clays. *Soc. Chem. Industry Jour.* 65, 298-304

445

446 Mark P. and Nilsson L. (2001) Structure and Dynamics of the TIP3P, SPC, and SPC/E Water Models at 298 K.
447 *J. Phys. Chem. A*. 105, 9954-9960.

448

449 Marry V., Dubois E., Malikova N., Breu J., and Haussler W. (2013) Anisotropy of water dynamics in clays:
450 Insights from molecular simulations for experimental QENS analysis. *J. Phys. Chem. C* 117, 15106-15115.

451

452 Michot L. J., Ferrage E., Jiménez-Ruiz M., Boehm M., and Delville A. (2012) Anisotropic features of water and
453 ion dynamics in synthetic Na- and Ca-smectites with tetrahedral layer charge. A combined quasi-elastic neutron-
454 scattering and molecular dynamics simulations study. *J. Phys. Chem. C* 116, 16619-16633.

455

456 Mosser-Ruck, R., Devineau, K., Charpentier, D., Cathelineau, M., 2005. Effects of ethylene glycol saturation
457 protocols on XRD patterns: a critical review and discussion. *Clays and Clay Minerals* 53, 631–638
458

459 Ortega-Castro J., Hernández-Haro N., Dove M.T., Hernández-Laguna A. and Saínz-Díaz C.I. (2010) Density
460 functional theory and Monte Carlo study of octahedral cation ordering of Al/Fe/Mg cations in dioctahedral 2:1
461 phyllosilicates. *American Mineralogist*, 95, 209-220
462

463 Plimpton S., (1995) Fast Parallel Algorithms for Short-Range Molecular Dynamics, *J Comp Phys*, 117, 1-19.
464

465 Reynolds R. C. (1965) An X-ray study of an ethylene glycol-montmorillonite complex. *Am. Min.* 50, 990-1001
466

467 Sato T., Watanabe T. and Otsuka R. (1992) Effects of layer charge, charge location, and energy change on
468 expansion properties of dioctahedral smectites. *Clays and Clay Minerals*. 40, 103-113
469

470

471

472 Środoń J. (1980) Precise identification of illite/smectite interstratification by X-ray powder diffraction. *Clay and*
473 *Clay Minerals*, 28, 401-411
474

475 Środoń J. (1981) X-ray identification of randomly interstratified illite/smectite in mixtures with discrete illite.
476 *Clay Miner.* 16, 297-304.
477

478 Środoń J. (1984) X-ray powder diffraction identification of illitic materials. *Clays & Clay Minerals* 32, 337-349.
479

480 Środoń J., Zeelmaekers E. and Derkowski A. (2009) The charge of component layers of illite-smectite in
481 bentonites and the nature of end-member illite. *Clays and Clay Minerals*. 57, 650-672.
482

483 Striolo A. (2011) From interfacial water to macroscopic observables: A Review. *Adsorption Science &*
484 *Technology* 29, 211-258.
485

486 Suter J. L. and Coveney P. V. (2009) Computer simulation study of the materials properties of intercalated and
487 exfoliated poly(ethylene)glycol clay nanocomposites. *Soft Matter* 5, 2239-2251.

488

489 Svensson P.D. and Hansen S. (2010) Intercalation of smectite with liquid ethylene glycol — Resolved in time
490 and space by synchrotron X-ray diffraction, *Appl. Clay Sci.* 48, 358 - 367

491

492 Teleman O., Jönsson B., and Engström S. (1987) A molecular dynamics simulation of a water model with
493 intramolecular degrees of freedom. *Molecular Physics* 60, 193 - 203.

494

495

496 **Figure captions**

497

498 **Figure 1.** Simulated basal spacing variability with increasing content of EG in EG/water-
499 smectite complex containing 0.8 H₂O/O₁₀(OH)₂.

500

501 **Figure 2.** ΔE of the glycolation reaction calculated for the water-smectite complex
502 containing 0.8 H₂O/O₁₀(OH)₂.

503

504 **Figure 3.** Radial distribution functions (RDF, left scale) and running coordination numbers
505 (RCN, right scale) calculated for: a) calcium atom – oxygen of EG (Ca-O_{EG}); b)
506 calcium atom – oxygen of water (Ca-O_w), in the structures of EG/water-smectite
507 complex containing 0.8 H₂O/O₁₀(OH)₂ with varying EG content.

508

509 **Figure 4.** Ca²⁺ coordination with (a) EG and (b) water in the interlayer space of smectite.

510

511 **Figure 5.** Simulated basal spacing variability with increasing water content in EG/water-
512 smectite complex containing 1.7 EG/O₁₀(OH)₂. Line is provided to guide the eye
513 only.

514

515 **Figure 6.** ΔE (kcal/mol) calculated for the reaction of hydration of the EG-smectite
516 complex. Line is provided to guide the eye only.

517

518 **Figure 7.** Radial distribution functions (RDF, left scale) and running coordination numbers
519 (RCN, right scale) calculated for: a) calcium atom – oxygen of EG (Ca-O_{EG}); b)

520 calcium atom – oxygen of water (Ca-O_w), in the structure of EG/water-smectite
521 complex containing 1.7 EG/O₁₀(OH)₂ with varying water content.

522

523 **Figure 8.** Atomic density profiles (arbitrary units) of calcium, carbon, oxygens of EG and
524 water obtained from MD simulations for bilayer EG/water-smectite complex with
525 different smectites: a) beidellite, charge = 0.3; b) beidellite, charge = 0.5; c)
526 montmorillonite, charge = 0.3; d) montmorillonite, charge = 0.5.

527

528 **Figure 9.** Atomic density profiles (arbitrary units) of calcium, sodium, potassium, carbon,
529 oxygens of EG and water obtained from MD simulations for bilayer EG/water-
530 smectite complex for a typical smectite substituted with different cations: a)
531 calcium; b) potassium; c) sodium.

532

533 **Figure 10.** Atomic density profiles (arbitrary units) of calcium, carbon, oxygen of EG and
534 water obtained from MD simulations for two-layer EG/water-smectite complex.
535 The distribution of EG and water atoms according to Reynolds (1965) is shown
536 for comparison as white/grey and black bars. The location of the smectite surface
537 is indicated by vertical dashed lines.

538

539 **Figure 11.** Atomic density profiles (arbitrary units) of calcium, carbon, oxygen of EG and
540 water obtained from MD simulations for one-layer EG/water-smectite complex.
541 The location of the smectite surface is indicated by vertical dashed lines.

542